

CHAPTER 2

STRUCTURAL CHARACTERIZATION OF
DEGRADATION DETERMINANT SIGNALS OF
YEAST AND MOUSE ORNITHINE
DECARBOXYLASE, IN ISOLATION FROM REST OF
THE PROTEIN SEQUENCES AND IN COMBINATION
WITH OTHER DEGRONS

According to 2.1Å crystal structure of human ODC, it consists of two domains: a TIM-like α/β barrel domain (residues 46-280) and a β -sheet domain (residues 7-45, 281-427) (Kern et al., 1999). Yeast ODC crystal structure is not available so far. Yeast and human ODC share 40% sequence homology (Figure 2.1) (Fonzi and Sypherd, 1987) while human and mouse ODC share 90.67% sequence homology.

Main aim of this study is to isolate DNA fragments encoding degrons of yeast and mouse ODC with the help of PCR amplification by using gene specific primers, clone them into bacterial expression vector, express and purify them in *E.coli* for structural characterization by circular dichroism and fluorescence spectroscopy.

2.2 Materials and methods

2.2.1 Strains and plasmids

E.coli DH5 α strain was used for cloning purpose. Bacterial expression vector pET30a (Novagene) was used for cloning and expression (Fig. 2.2). Expression and purification of protein were done using *E.coli* BL21(DE3) strain. All the bacterial cultures were grown in Luria–Bertani medium (Himedia) and under antibiotic selection of 100 μ g/ml ampicillin and 50 μ g/ml kanamycin, depending on the necessity. Bacterial transformations were done with calcium chloride method (Cohen and Kelly, 2003). Details of all the strains and plasmids are described in Table 2.1.

2.2.2 Construction of chimeric plasmids

DNA fragments encoding amino acid sequences representing degrons of yODC and mODC have been cloned in pET30a vector downstream to 6X-His tag by using different restriction sites for the purpose of structural studies (figure 2.1). Restriction digestions and ligations were done using standard methods (Sambrook, 1989). The

oligonucleotide primers used in this study were mentioned in Table 2.2. All the constructs were finally confirmed by DNA sequencing.

Table 2.1 Strains and plasmids used in this study

Strains and Plasmids	Details	Protein Molecular weight (kDa)
<i>E.coli</i> DH5 α	F ⁻ <i>endA1 glnV44 thi-1 recA1 relA1 gyrA96 deoR nupG</i> Φ 80 <i>dlacZ</i> Δ M15 Δ (<i>lacZYA-argF</i>)U169, <i>hsdR17</i> (r _K ⁻ m _K ⁺), λ ⁻	
<i>E.coli</i> BL21(DE3)	F ⁻ <i>ompT gal dcm lon hsdS_B</i> (r _B ⁻ m _B ⁻) λ (DE3 [<i>lacIIacUV5-T7 gene 1 ind1 sam7 nin5</i>])	
pET30a	Bacterial expression vector with N-terminal his tag	
pET-N50	First 50 residues of yODC	11.1
pET- α/β	α/β barrel domain of yODC	39.3
pET-N α/β	N-terminal domain of yODC	43.5
pET-AzBE	Expressing yeast ODC antizyme binding element (AzBE) peptide	11.1
pET-mODC	Expressing mouse ODC last 37 residues	9.3
pET- α/β -mODC	Expressing yeast ODC α/β peptide with mouse ODC last 37 residues	43.2
pET-AzBE-mODC	Expressing yeast ODC antizyme binding element (AzBE) with mouse ODC last 37 residues	15.9
pET-N50-mODC	Expressing first 50 amino acid of yeast ODC with mouse ODC last 37 residues	14.8

Table 2.2 List of oligonucleotide primers used in this study. Bold letters indicate restriction sites.

Structural study	Primer sequences
AzBE FR	5'-GCG GAATTC AAACATCTCGCCGGATAG-3'
AzBE RE with stop codon	5'-ATG AAGCTT TCAGGTAGAGTCATCGGTAGC-3'
AzBE RE without stop codon	5'-ATG AAGCTT GGTAGAGTCATCGGTAGC-3'
mODC FR	5'-GAAA AAGCTT GC TTC CCG CCG GAG GTG-3'
mODC RE	5'-GGG CTCGAG CTACACATTGATCCTAGCAGA-3'
α/β FR	5'-AAT GGATCC CACAATCTTTTGCTTGA ACTAAAG-3'
α/β RE without stop codon	5'-ATAG GAGCTC TGCTTCATTCTCAGACAGTTT-3'
N50 FR	5'-TAT GGATCC ATGTCTAGTACTCAAGTAGGAAAT-3'
N50 RE without stop codon	5'-ATAACAG GAGCTC TCCAAATCTTGGTTATTCTTTAGTTCAA-3'

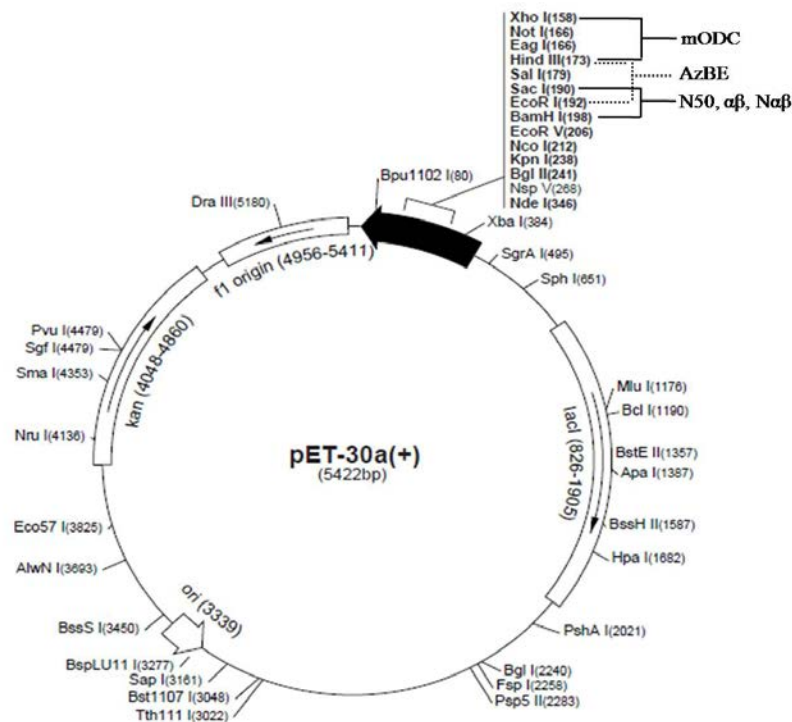


Figure 2.2 Vector map of pET30a. Restriction sites used to insert DNA sequences encoding degrons

Table 2.3 Information about cloning of chimeric constructs

Construct	Size of DNA fragment	Restriction sites used for cloning	Expected size of DNA after amplifying with vector specific primers(T7 primers)
pET30a	--	--	413 bp
pET-N50	150 bp	<i>Bam</i> HI- <i>Sac</i> I	557 bp
pET- α/β	924 bp	<i>Bam</i> HI- <i>Sac</i> I	1331 bp
pET-N α/β	1038 bp	<i>Bam</i> HI- <i>Sac</i> I	1441 bp
pET-AzBE	180 bp	<i>Eco</i> RI- <i>Hind</i> III	580 bp
pET-mODC	114 bp	<i>Hind</i> III- <i>Xho</i> I	518 bp
pET- α/β -mODC	1038 bp	<i>Bam</i> HI- <i>Xho</i> I	1431 bp
pET-AzBE-mODC	294 bp	<i>Eco</i> RI- <i>Xho</i> I	679 bp
pET-N50-mODC	264 bp	<i>Bam</i> HI- <i>Xho</i> I	643 bp

2.2.3 Expression and purification of proteins

Fusion proteins of His-tagged degrons were over-expressed in *Escherichia coli* BL21 (DE3) cells. Freshly transformed cells were grown in Luria–Bertani medium (Himedia) containing 50 μ g/ml kanamycin at 37 °C upto 0.5 OD at 600nm, at which point protein expression was induced with 1 mM isopropyl β -D-1-thiogalactopyranoside (IPTG). Cells were further allowed to grow for an additional 4 h at 37 °C, the cells were pelleted at 8000g for 3 min at 4 °C and resuspended in washing buffer A (50 mM sodium phosphate ,500 mM NaCl, 20 mM imidazole, pH 8) with protease inhibitor cocktail. The cells were lysed by sonication and the lysate was centrifuged at 12000g for 15min at 4°C to remove cell debris. His-tagged degrons were purified from the supernatant via immobilized affinity chromatography by using Ni-NTA agarose resin (Qiagen) (Fig. 2.3). Briefly, the lysate was incubated with resin for 1hr, washed the resin with 10 column volumes of washing buffer A, and eluted the tagged protein with elution

buffer containing 500 mM imidazole (pH 8). Further dialysis the protein against 10mM sodium phosphate buffer, pH 8 has been carried out to remove imidazole and other salts. The purity of sample was checked by sodium dodecyl sulphate polyacrylamide gel electrophoresis (SDS-PAGE) (Laemmli, 1970).

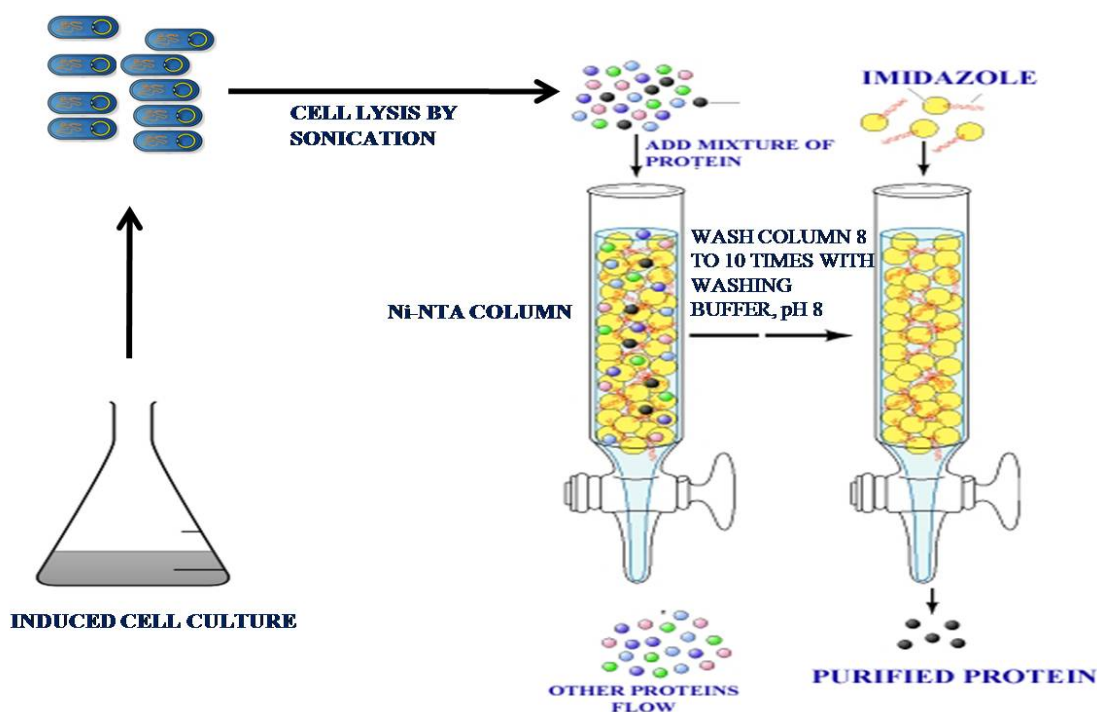


Figure 2.3 Strategy for purification of His-tagged peptides by Ni-NTA affinity chromatography

2.2.4 Structural characterizations

Circular dichroism and fluorescence spectroscopy were carried out to know the structural integrity of isolated peptides of yeast and mouse ornithine decarboxylase. Lab standard protocols were used for this study (Mishra et al., 2011; Mishra et al., 2009; Ratnaprabha and U. Sasidhar, 1998; Sasidhar and Prabha, 2000).

2.2.4.1 Circular dichroism study

Far UV-CD spectra were recorded in the range of 195-250nm (Jasco-J-815). Purified 30uM proteins in 10mM phosphate buffer were loaded into CD. 1mm path

length cell was used. Data pitch was 1nm and scan speed was 50nm/sec. The CD spectra shown are the average of 3 scans. Normalized the blank with 10mM phosphate buffer. The percentage of secondary structure was calculated by using CDPro software (Sreerama and Woody, 2000).

Secondary structure of peptides was inducing by addition of 40% trifluoroethanol (TFE). Proper blanks were prepared for all the samples and the spectra of the samples were blank corrected.

2.2.4.2 Fluorescence spectroscopy

Hitachi FL-7000 fluorimeter was used to record fluorescence spectra of purified peptides. Peptides were excited at 280nm and record emission in between 300-400nm wavelength. Slit width was 5 nm. Protein concentration was 5 μ M. Protein solutions were prepared in phosphate buffer, pH 8.0.

To determine the tertiary conformation of peptides, guanidine hydrochloride denaturation study was carried out. Peptides were denatured with increasing concentration of guanidine hydrochloride (0.6 to 6M). Proper blanks were prepared and the spectra shown in the result are blank corrected.

1-Anilino 8-naphthalene sulphonic acid (ANS) was used as an extrinsic fluorophore at a concentration of 50 μ M in fluorescence resonance energy transfer(FRET) study. Protein solution having 50 μ M ANS was excited at 280nm and emission was recorded between 300 and 550 nm. Remaining parameters are same.

2.2.5 Homology modeling of degrons peptides

The sequences of yeast and mouse ODC peptides alone and in combination were submitted to I-TASSER server for 3Dstructure prediction(Roy et

al., 2010; Yang et al., 2015; Zhang, 2008). The output of I-TASSER was submitted to PyMOL program to view the 3D structure of the peptides (DeLano, 2010).

2.2.6 N50 structure characterization

AGADIR algorithm was used for predicting the sequence with high α -helical propensity in N50 peptide (Munoz and Serrano, 1994). Helical wheel diagram was drawn in <http://rzlab.ucr.edu/scripts/wheel/wheel.cgi> online server.

2.3 Results

2.3.1 Cloning of deignons of yeast and mouse ornithine decarboxylase (alone and in combination) in bacterial expression vector

Gene fragments corresponding to yODC deignons N50, α/β and N α/β was successfully amplified from pRS314 containing yeast ODC gene and fragment of gene coding for last 37 amino acids of mouse ODC (CmODC) was successfully amplified from pBSKS-mODC vector carrying entire mouse ODC gene (Fig. 2.4).

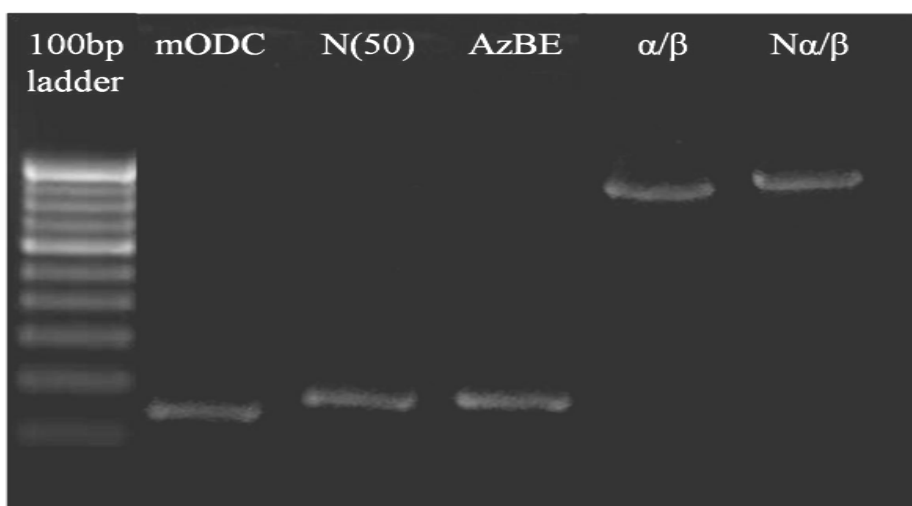


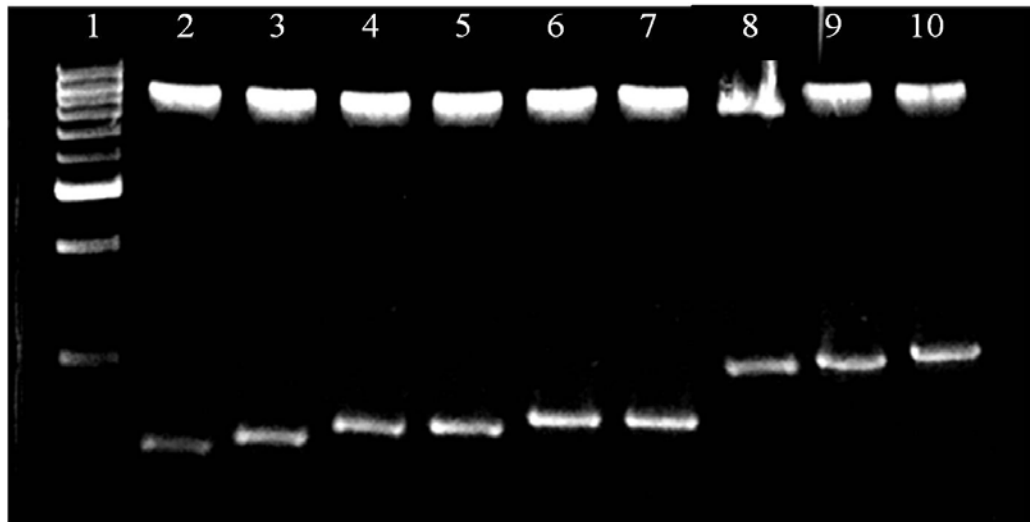
Figure 2.4 PCR amplicons of different fragments of ODCs representing deignons by using gene specific primers.

After successfully getting PCR amplicons encoding degron of ODCs (Fig. 2.4), they were cloned into pET30a bacterial expression vector alone and in combination with each other. Constructs made in the lab earlier, N50, α/β and N α/β were used for further structural characterization (Swapnali Kulkarni's thesis, 2012). Remaining chimeric constructs were prepared in this study and their cloning information has been given in Table 2.3.

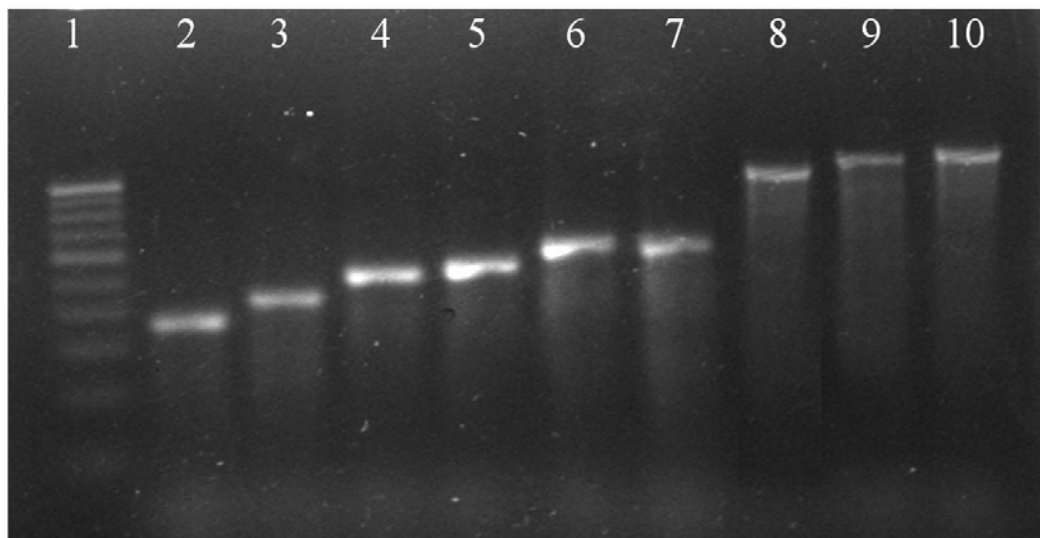
Positive constructs were confirmed by double digestion of the plasmids with *Bam*HI and *Xho*I restriction enzymes (Fig. 2.5 A) and the sizes of PCR products after amplifying with vector specific primers were confirmed (Fig. 2.5 B). All the constructs were finally confirmed by DNA sequencing.

2.3.2 Expression and purification of degron peptides of ODCs

All chimeric constructs of peptides of ODCs were transformed in *E.coli* BL21 (DE3) strain for protein expression and purification. Fig. 2.6 shows protein expression (A) and purification profile (B&C) of ODCs peptides. Details of peptides were mentioned in Table 2.1.



(A)



(B)

Figure 2.5 Confirmation of all constructs cloned in this study.

(A) Insert release of positive transformant after digested with *Bam*HI and *Xho*I restriction enzymes. Lane 1 shows 1kb DNA ladder, Lane2 to 10 shows insert release of epET, mODC, N50, AzBE, N50-mODC, AzBE-mODC, α/β , α/β -mODC and $N\alpha/\beta$ respectively.

(B) Compare the size of positive clones PCR amplicon by using T7 primers. Lane 1 shows 100 bp DNA ladder, Lane2 to 10 shows PCR amplicons of epET, mODC, N50, AzBE, N50-mODC, AzBE-mODC, α/β , α/β -mODC and $N\alpha/\beta$ respectively.

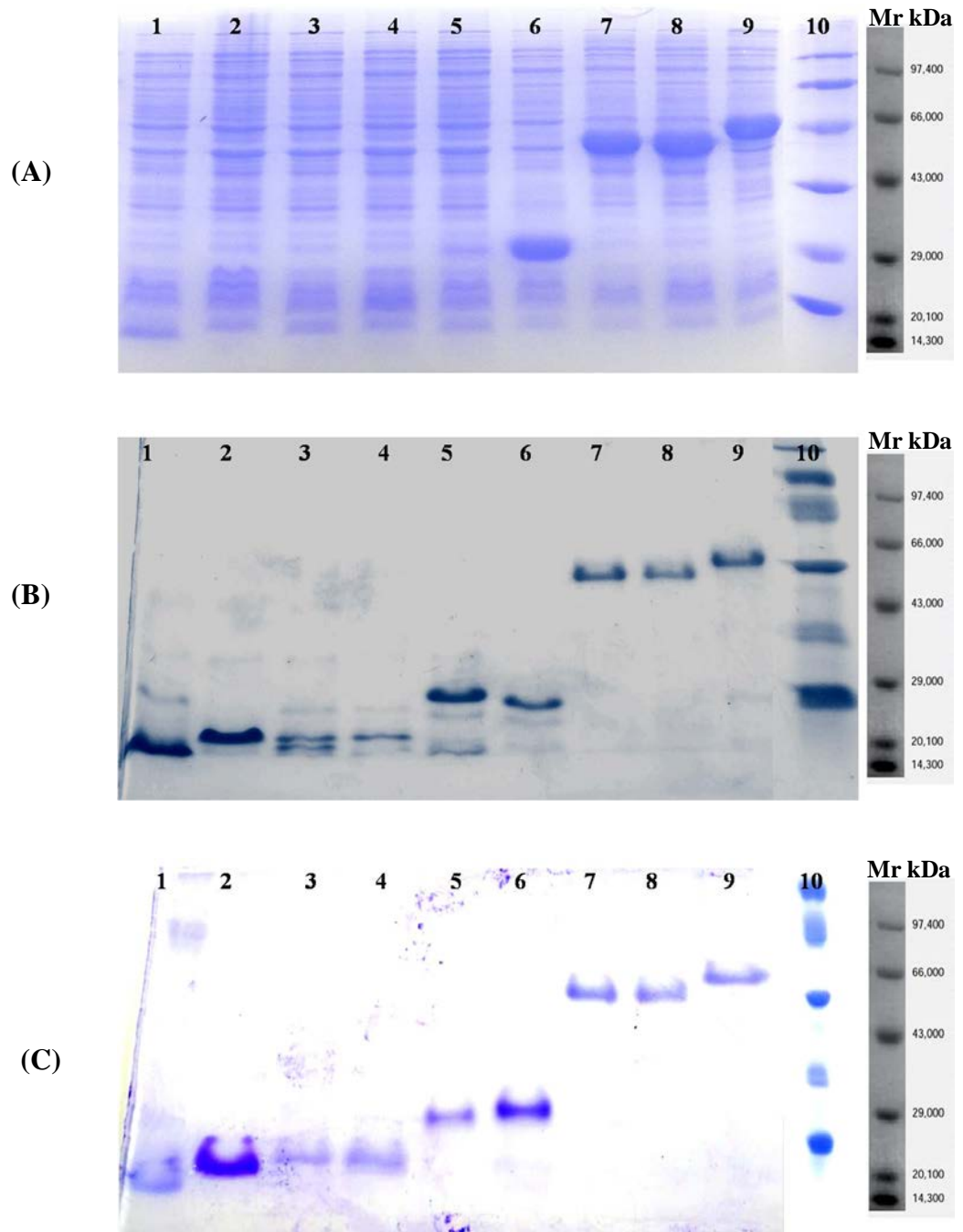


Figure 2.6 SDS-PAGE gel representing the expression and purification of degnon peptides

(A) SDS-PAGE gel showing expression profile of selected degnons of ODCs, (B&C) Purification of degnon peptides of ODCs by affinity chromatography.

Lane 1 to 9 are demonstrating pET expressing His-tag, mODC, N50, AzBE, N50-mODC, AzBE-mODC, α/β , α/β -mODC and $N\alpha/\beta$ peptides respectively and Lane 10 shows protein molecular weight marker.

2.3.3 Structural characterizations of N50, α/β and N α/β peptides

Earlier in our lab, structural studies of N50, α/β and N α/β have been done by fluorescence spectroscopy and circular dichroism techniques (Swapnali Kulkarni's thesis, 2012). In continuation to the previous work, further structural characterization of same peptides was carried out in this study. We wanted to determine if there is any correlation between the degradation efficiency of peptides and their structure. For that, far UV CD spectra were recorded for the peptides N50, α/β and N α/β to understand the nature and content of secondary structure in buffer and 40% TFE (2,2,2 - trifluoroethanol) (Fig. 2.7).

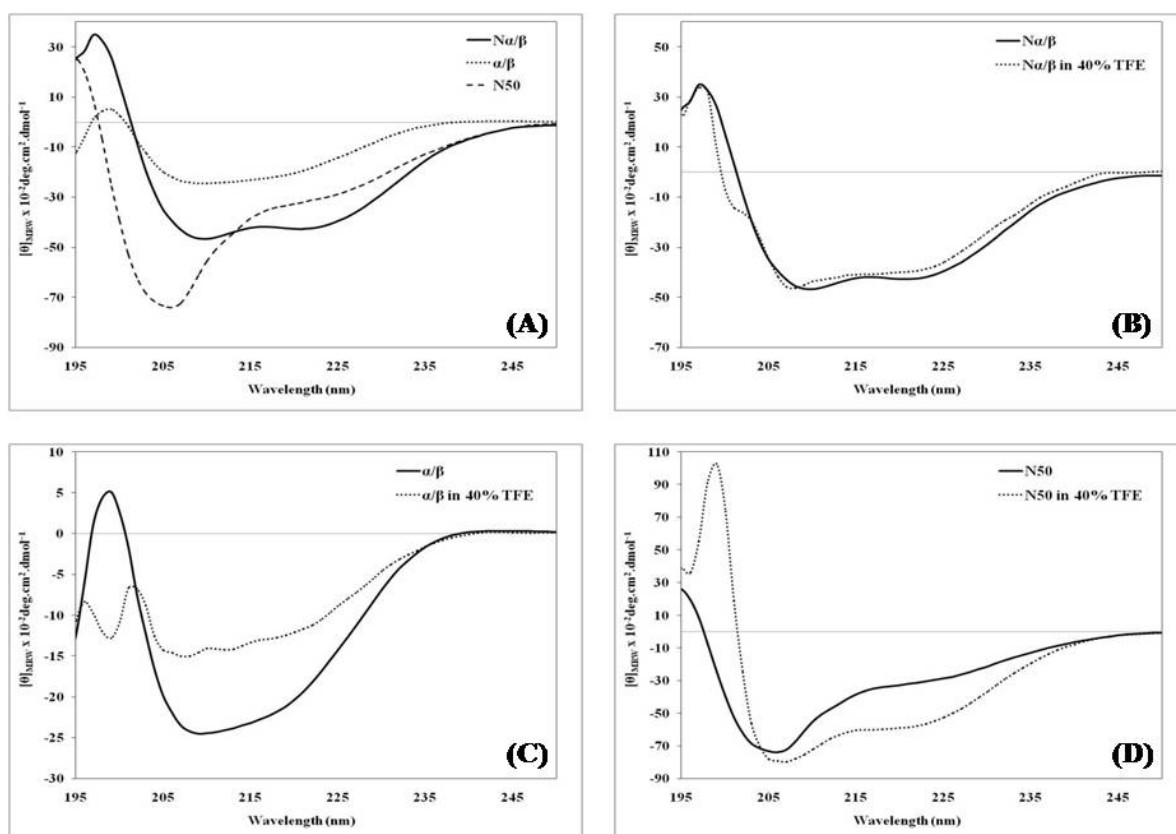


Figure 2.7 Far UV CD spectra of the peptides N α/β , α/β and N50

(A) Overlay far UV CD spectra of the peptides N α/β , α/β and N50 in 10mM Tris buffer, pH 8.0, recorded from 195 nm to 250 nm to analyze the secondary structure status of the peptides. (B), (C) and (D) Far UV CD spectra in buffer (-) and in 40% TFE (--) of the peptides N α/β , α/β and N50 respectively.

The results showed a well formed α/β structure in the case of $N\alpha/\beta$. However, the spectrum of α/β peptide displayed β sheet character as its dominant feature. The degran character of the N-terminal 44 residues termed as ODS was reported earlier with a assumption that the N-terminal is unstructured (Godderz et al., 2011). However, no studies are available on the structure of N-terminal extension and for the first time structural characterization of N50 was attempted in this study. Interestingly, the far UV CD spectrum of N50 showed negative ellipticity values at 207 nm and 222 nm. From an earlier study it is known that if the ratio of ellipticities observed at 222 nm and 207 nm corresponds to a value of 0.4, then the structure formed is a 3_{10} helix (Manning and Woody, 1991). With N50 the value observed was 0.418, suggesting the presence of 3_{10} helix (table 2.4). Besides, the analysis of CD spectra using CD Pro indicated the various components of secondary structure in all the three peptides (Table 2.4).

Table 2.4 Secondary structural analysis of far-UV CD spectra of the peptides N50, α/β and $N\alpha/\beta$ using CD Pro software

Referenceset: SP43	Helix (%)	Sheet (%)	Turn/ Unread (%)	Value of 222nm/207nm
$N\alpha/\beta$	30.8	18.6	49.4	$-29.1053/-31.4667 =$ 0.924956
α/β	17.7	27.9	54.4	$-19.7572/-26.1444 =$ 0.755695
N50	32.3	16.6	50.2	$-15.7254/-37.5568 =$ 0.41871

The above result led to the question that whether the conformations displayed by these peptides are optimal or there are regions in the peptides which have weak propensity for adopting secondary structure, but are remaining extended under the

experimental conditions. With the aim of answering the question, far-UV CD spectra of the degran peptides was recorded in presence of 40% TFE (2,2,2 - trifluoroethanol), a solvent known to stabilize α -helical structure in peptides which can form α -helices under ideal conditions, but remain in extended conformations otherwise. From the results presented in Fig. 2.7B, it is clear that N α/β does not show any change in the structure, establishing that its α -helical regions are completely folded and addition of TFE did not have any influence over the secondary structure of the fragment. The α/β fragment showed a change in its secondary structure (Fig. 2.7C). However, the result observed with N50 was surprising as long stretches of 3_{10} helix are uncommon to proteins in their native state. To test if the above result is a pointer towards α -helical propensity of the peptide, CD spectrum of N50 was recorded in the presence of TFE. The peptide readily adopted α -helical conformation (Fig. 2.7D).

2.3.4 Structural characterizations of AzBE, mODC, AzBE-mODC, N50-mODC and α/β -mODC

As mentioned earlier in chapter 1, many structured and unstructured regions are present within ODC which help to make it a better substrate for antizyme mediated proteasomal degradation. In this study, structure of AzBE, mODC, AzBE-mODC, N50-mODC and α/β -mODC were characterized by circular dichroism and fluorescence spectroscopy.

2.3.4.1 Circular dichroism study

To determine the secondary structure content of the peptides AzBE, mODC, AzBE-mODC, N50-mODC and α/β -mODC, far UV CD spectra were recorded in buffer (pH 8) and in presence of 40% TFE (Fig. 2.8).

The far UV CD spectra of N50-mODC and α/β -mODC show a negative hump at 208 nm and small negative shoulder at 222 nm indicating presence of α -helical structure (Fig. 2.8 D&E) and after addition 40% TFE, both the chimeric peptides have adopted strong helical conformation. As mentioned earlier N50 peptide has 3_{10} helix like conformation, while α/β peptide contains more β -sheet content but after fusion with mODC, both the peptides N50-mODC and α/β -mODC have adopted helical conformation.

While far UV CD spectra of AzBE, mODC and AzBE-mODC did not shown any signature pattern of secondary structure, after addition of 40% TFE secondary structure was induced in all the cases (Fig. 2.7 A,B&C). The reason behind this observation could be that AzBE is a small fragment of α/β domain of yeast ODC. So, it may not be able to maintain its structure without rest of the protein. It was reported that last 37 residues of mammalian ODC (CmODC) is unstructured (Almud et al., 2000; Kern et al., 1999). Our results support this observation. Further, CD Pro software was used to calculate secondary structure content for all the peptides (Table 2.5).

Table 2.5 CD Pro analysis of far UV CD spectra of peptides AzBE, mODC, AzBE-mODC, N50-mODC and α/β -mODC

Referenceset: SP43	Helix (%)	Sheet (%)	Turn/ Unread (%)
AzBE	4.7	35.9	58.5
mODC	17.5	30.6	51.6
AzBE-mODC	2.8	36.6	58.1
N50-mODC	32.8	21	47
α/β -mODC	15.2	45.4	39.4

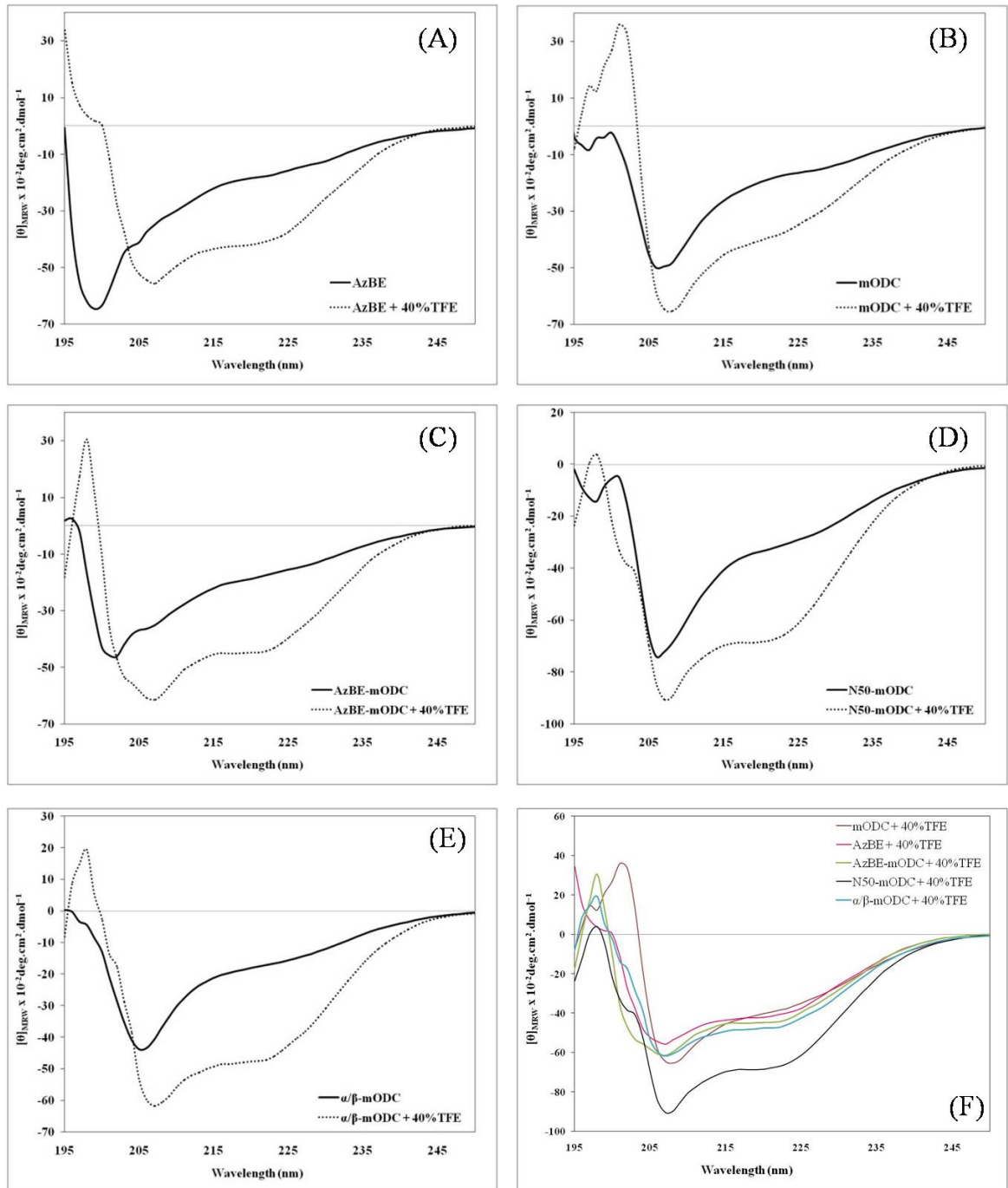


Figure 2.8 Far UV circular dichroism spectra of peptides AzBE (A), mODC (B), AzBE+mODC (C), N50+mODC (D), and α/β +mODC (E) in phosphate buffer, pH 8 (—) and in the presence of 40% TFE (---). Panel (F) is overlay of far UV CD spectra of all selected peptides in the presence of 40% TFE.

2.3.4.2 Fluorescence spectroscopy

After isolating degran peptides from host protein, to find answer to the question that whether they can fold independently without rest of the protein, fluorescence spectra of AzBE, mODC, AzBE-mODC, N50-mODC and α/β -mODC were recorded by changing the solvent conditions: 1) in guanidine hydrochloride and in urea and 2) fluorescence resonance energy transfer (FRET) using the extrinsic fluorophore ANS.

2.3.4.2.1 Guanidine hydrochloride and urea denaturation analysis

Guanidine hydrochloride (GdmCl) and urea are denaturing agents (chaotropic agents) causing loss of secondary and tertiary structure in proteins. The peptides have been denatured with increasing concentrations of guanidine hydrochloride. Change in fluorescence intensity and shift in λ_{max} were observed in the emission spectra. This is due to change in extent of exposure of aromatic amino acids to aqueous environment due to changes in peptide structure. Peptides were excited at 280nm and the emission were recorded between 300-400nm wavelength (Fig. 2.9).

Fig. 2.9 is clearly indicating that α/β -mODC peptides are changing their fluorescence intensity with respect to increase in guanidine hydrochloride concentration. The emission spectra of α/β -mODC shows increase in fluorescence intensity when guanidine hydrochloride concentration was raised (Fig. 2.9E). In the native form aromatic amino acids are buried resulted low fluorescence intensity after denaturation they are exposed showing more fluorescence intensity.

The spectra of AzBE, CmODC, AzBE-CmODC and N50-CmODC confirm that the peptides lack tertiary structure due to their small size.

Same results were obtained in urea denaturation study for all the peptides (Fig. 2.10). These fluorescence spectroscopic observation support the result obtained with circular dichroism study (Fig. 2.8).

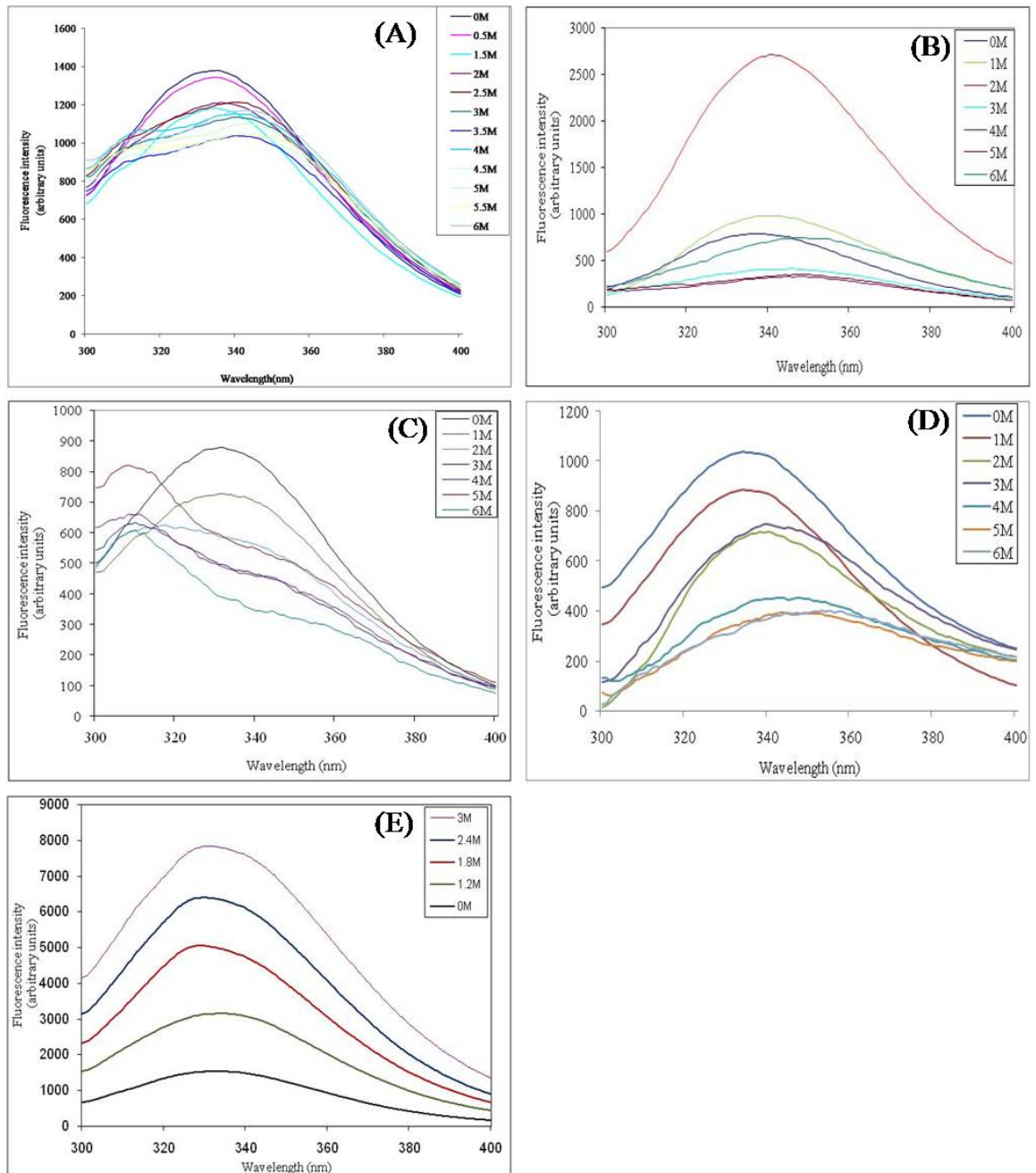


Figure 2.9 Guanidine hydrochloride denaturation curve of degran peptides of ODCs

(A) AzBE, (B) mODC, (C) AzBE-mODC, (D) N50-mODC and (E) α/β -mODC

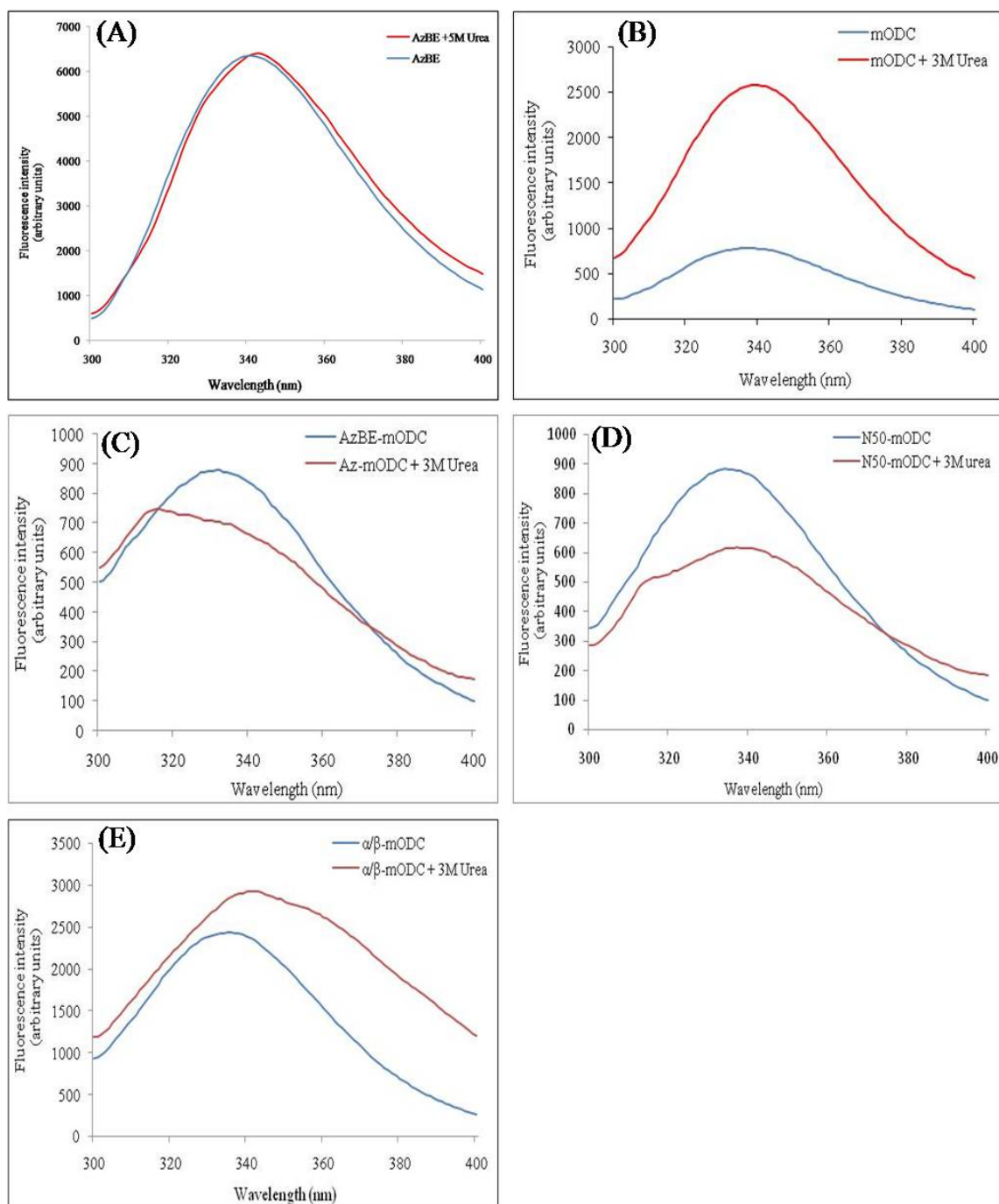


Figure 2.10 Fluorescence emission spectra of peptides of ODCs after denaturation with urea

(A) AzBE, (B) mODC, (C) AzBE-mODC, (D) N50-mODC and (E) α/β -mODC

2.3.4.2.2 Fluorescence Resonance Energy Transfer (FRET)

In FRET, the energy is transferred from one fluorophore to another fluorophore provided the emission wavelength of the first fluorophore overlaps the excitation wavelength of the second fluorophore and they are within a distance of 10-100Å. In this study, 1-Anilino 8-naphthalene sulphonic acid (ANS) is used as an extrinsic fluorophore. ANS is known to bind to the exposed hydrophobic surfaces of proteins. It shows higher fluorescence in hydrophobic environment compared to hydrophilic environment. The excitation wavelength of ANS is 350 to 380nm and emission wavelength is 520nm. Purified peptides were excited at 280nm with and without ANS and emission spectra were recorded between 300 to 550nm.

The FRET spectra of α/β -mODC and N50-mODC show energy transfer between aromatic amino acids to ANS (Fig. 2.11D&E). It means that these peptides contain more exposed hydrophobic surface in their native structure. In remaining peptides AzBE, mODC and AzBE-mODC FRET spectra were not showing any energy transfer. Possible reasons behind this observation is that the peptides AzBE, mODC and AzBE-mODC are contain made up of polar amino acid residues as they are exposed to surface in native protein.

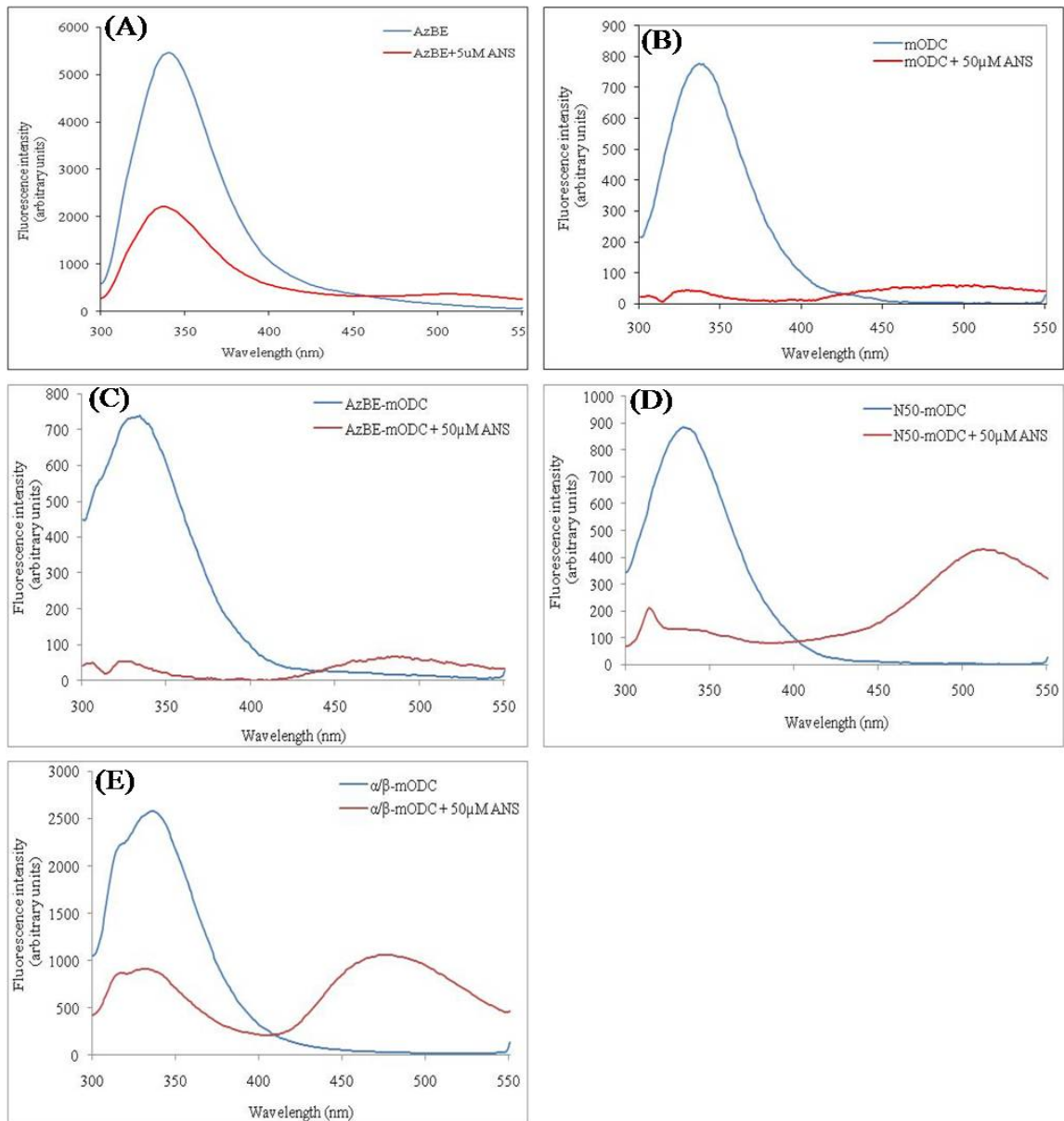


Figure 2.11 Fluorescence Resonance Energy Transfer (FRET) of deignons of ODCs
 (A) AzBE, (B) mODC, (C) AzBE-mODC, (D) N50-mODC, (E) α/β -mODC

2.3.5 Homology modeling for deignons of ODCs

I-TASSER, online server used to generate homology models for deignons peptides sequence. Fasta sequence of all selected peptides has been submitted to I-TASSER server. Output of server gave various model among them was high confidence score (C-score) and maximum % of similarity with template used to predict structure

have been selected. The output of I-TASSER was submitted to PyMOL program to view the 3D structure of the peptides. 3D modeling of α/β , $N\alpha/\beta$ and α/β -mODC using I-TASSER resulted in TIM like α/β barrel structure. The models of the selected degnons peptides generated using Pymol are presented in Fig. 2.12. The 3D model of structure generated indicates structural preference of the sequence rather than the exact content of secondary structure. Since, α/β , $N\alpha/\beta$ and α/β -mODC have a large overlap in their sequences; they display almost similar contents of helix and sheet. Moreover, with $N\alpha/\beta$ peptide interactions between regions of N50 and α/β domain were observed (Table 2.6).

Table 2.6 Polar interactions of N50 region with α/β region in $N\alpha/\beta$ structure

Backbone- backbone		Backbone – side chain	Side chain - side chain
Y31-C=O...H-N-G35	H39-C=O...H-N-L43	T14-C=O...H-N-K96	E57-C=O...H-N-K28
K33-C=O...H-N-T37	N40-C=O...H-N-E44	L130-C=O...H-O-T15	Q49-C=O...H-O-T121
D34-C=O...H-N-L38	N40-C=O...H-N-L43	G93-C=O...H-O-T16	K29-N-H...O-T26
G35-C=O...H-N-H39	L41-C=O...H-N-L45	K28-N-H...O=C-E57	K33-N-H...O=C-E36
E36-C=O...H-N-H39	L42-C=O...H-N-L45	Y31-C=O...H-N-H56	N22-C=O...H-N-N8
E36-C=O...H-N-N40	L42-C=O...H-N-K46		D19-C=O...O-H-S11
T37-C=O...H-N-L41	L43-C=O...H-N-N47		K46-N-H...O=C-D50
L38-C=O...H-N-L42	T14-N-H...O=C-L126		T14-O-H...N(H)-K96
			K28-N-H...O=C-E57 (2 interactions)
			Q49-C=O...H-O-T121

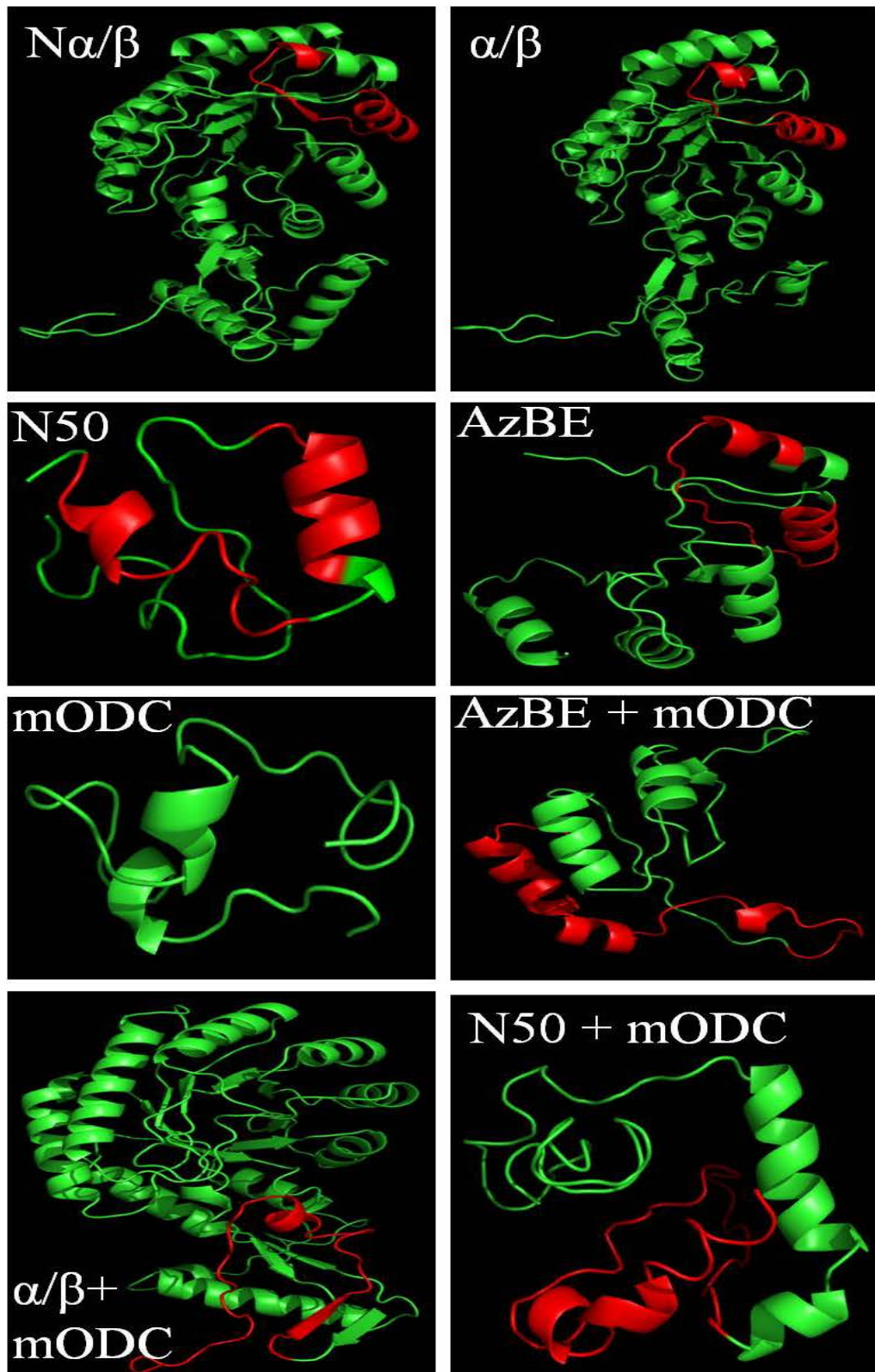


Figure 2.12 Homology modeling of peptides representing degrens of ODCs

2.3.6 Theoretical sequence analysis of first 50 residues of yeast ODC (N50)

When the helical propensity of N50 peptide was observed in far UV CD spectra, AGADIR algorithm has been used to find whether the entire sequence or a part of it takes up helical structure in N50 sequence. AGADIR predicts the helical behaviour of monomeric peptides. AGADIR calculations carried out on entire sequence of N50 sliding a window of 7 residues (like 1-7, 2-8, 3-9....44-50). Output results indicated the sequence ‘**31YYKDGETLHNLLLELKNN48**’ showed greater preference for helical structure over rest of the peptide sequence (Fig. 2.13A&B). As mentioned earlier 3D modeling of the same peptide was carried out on I-TASSER server. The somewhat hyphenated occurrence of hydrophobic and polar residues suggested a possibility of amphipathic α -helix. To check this possibility helical wheel diagram has been drawn which has supported formation of amphipathic α -helix as a side of the helix has four hydrophobic residues and the other side has polar residues (Fig. 2.13C).

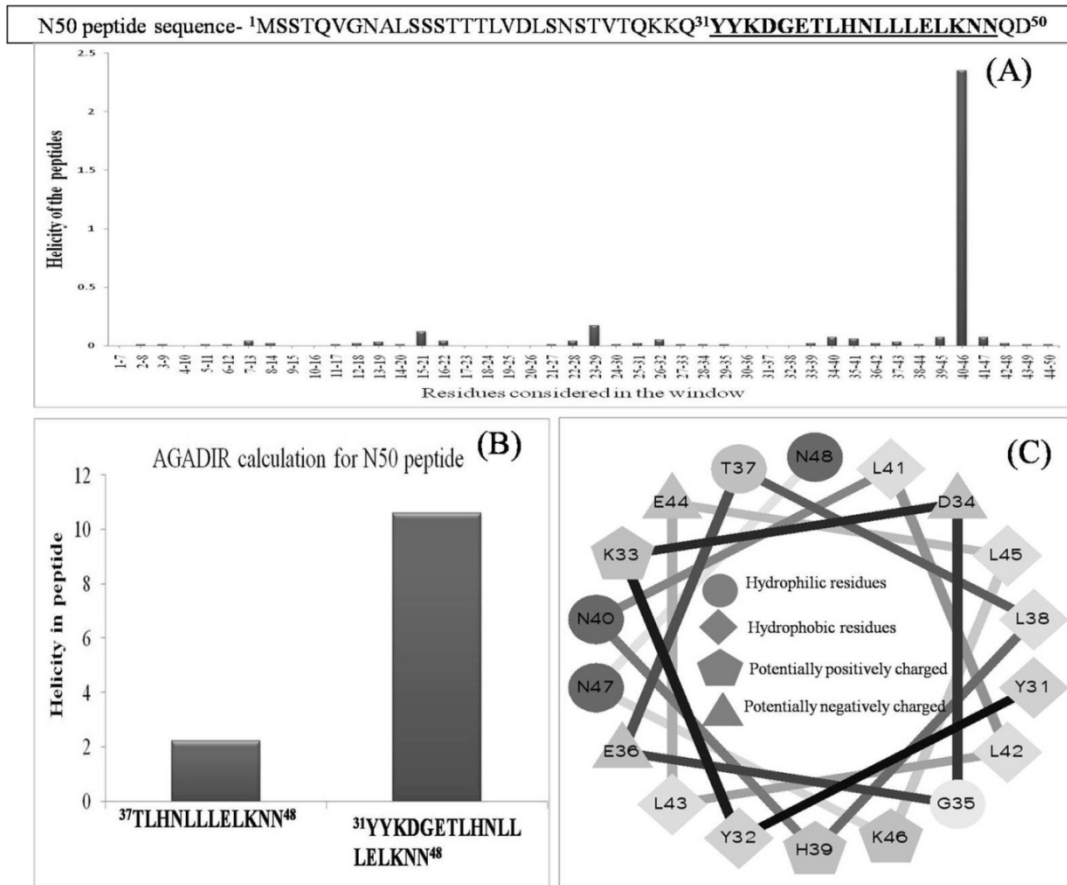


Figure 2.13(A) AGADIR calculations carried out on the entire sequence of N50 sliding a window of 7 residues. **(B)** The sequences with helical propensity in N50 is shown. **(C)** Wheel diagram of the peptide '31YYKDGETLHNLLLELKNN48', showing amphipathic nature.

2.4 Discussion

X-ray crystallographic structures of ODC from mouse and human revealed that the enzyme has two domains in its structure (Almud et al., 2000; Kern et al., 1999). On the other hand, structure of yeast ODC (yODC) has not been resolved using NMR spectroscopy or X-ray crystallography. Yeast ODC and mammalian ODC (mODC) share 40% sequence homology (Fonzi and Sypherd, 1987). However, in yeast ODC there is an extension of 50 amino acid residues in the N-terminal and in the mammalian ODC

the C-terminal has a tail of 37 residues with extended structure, which do not have an equivalent in the other protein.

From circular dichroism study, it is clear that N α / β degrons able to gain well stable α - helical structure. While CD spectrum of α / β has more β -sheet and less α -helix content than N α / β . Moreover, addition of TFE made no difference to secondary structure of N α / β , establishing that it has already folded into its optimal and most stable conformation. α / β fragment, in contrast to N α / β has greater β -sheet content and showed a change in secondary structure in TFE, indicating that its α -helix has not folded to its optimal content. However, the result observed with N50 was surprising as long stretches of 3_{10} helix are uncommon to proteins in their native state and the peptide readily adopted α -helical conformation in presence of TFE. As mentioned earlier the degradation potential of ODS was reported by Godderz et al. in 2011(Godderz et al., 2011), while the present work was underway. Further the authors made a comment that the peptide is unstructured. ODS which represents the first 44 residues of N-terminal of ODC shares some commonality with the N50 peptide reported here. Structure prediction with the sequence of N50 using I-TASSER and AGADIR algorithm suggested a strong possibility for existence of α -helical conformation between amino acid residues 31 to 48. ODS does not have some of the residues which formed part of α -helix in our model of N50. Furthermore, the interactions observed in our model between first 20 residues of the N-terminal and the α / β domain. Overall, these result established that first 50 residues of yeast ODC help to maintain whole N-terminal domain structure.

α / β -mODC is a chimeric fusion of yeast α / β degrons and last 37 residues of mouse ODC. CD spectrum of α / β -mODC was showing mix α / β like structure and in TFE it shows more α -helix. Yeast α / β peptide contains more β -sheet content, after fusion

with mODC it adopts helical conformation. These observations suggest that α/β peptide needs supportive residues at N-terminal or at C-terminal to take up their native conformation, which means that yeast α/β peptide in isolation has β -sheet structure. After addition of N50 at N-terminal as in N α/β or mODC at C-terminal as in α/β -mODC, the sequence of α/β adopts more stable α/β structure. From fluorescence spectra, it was found that chimeric peptide α/β -mODC takes up tertiary conformation.

Degrans AzBE, mODC, AzBE-mODC and N50-mODC failed to adopt secondary as well as tertiary conformation in buffer. Secondary structure was induced in presence of TFE.

Homology modeling of α/β , N α/β and α/β -mODC resulted in α/β structure. Moreover, with N α/β peptide, interactions were observed in between regions of N50 and α/β domain in modeling study. Predicted 3D structure of remaining degrons has shown more α -helical content. There are differences between the values of secondary structures obtained by CD spectra and 3D modeling. The values observed for various secondary structural features with CD spectra are closer to reality. I-TASSER uses fold recognition to detect structure templates from the protein data bank for a given sequence. Hence, the 3D model of degrons has indicated structural preference of the sequence rather than the exact content of secondary structure.

In conclusion, this study establishes that the degrons N50 and N α/β from yeast ornithine decarboxylase take up secondary structure independent of rest of the protein. Moreover, this study has changed the earlier assumption regarding N50 that it is not unstructured region, it has secondary structure. It has also established that N50 region helps to maintain structural integrity of N-terminal domain of yeast ODC. Structural studies of chimeric constructs have established that combination of two fragments from

different host proteins can maintain their structural content even expressed in fusion protein.